

A new anti-cancer strategy of damaging mitochondria by pro-apoptotic peptide functionalized gold nanoparticles†

Cite this: *Chem. Commun.*, 2013, **49**, 6403

Received 3rd May 2013,
Accepted 4th June 2013

DOI: 10.1039/c3cc43283a

www.rsc.org/chemcomm

Wei-Hai Chen,^{‡a} Jing-Xiao Chen,^{‡a} Han Cheng,^{‡a} Chang-Sheng Chen,^a Juan Yang,^a Xiao-Ding Xu,^a Yan Wang,^b Ren-Xi Zhuo^a and Xian-Zheng Zhang^{*a}

Gold nanoparticles functionalized with pro-apoptotic peptide (PAP-AuNPs) were fabricated, which were able to lead to programmed cell-death by damaging mitochondria.

Chemotherapy has been widely used to treat cancer, but chemotherapy drugs may also cause serious side effects. The targeted drug delivery to a particular intracellular site will dramatically improve its therapeutic effect and reduce the side effect.¹ In particular, subcellular drug delivery systems can potentiate the therapeutic effect, and kill cancer cells more directly and efficiently.² Subcellular organelles, such as the nucleus and mitochondria, are of importance in cancer treatment because the damage of these organelles will lead to irreversible cell apoptosis.³ Particularly noteworthy are the mitochondria, which not only regulate calcium and redox signalling, but control cell death. With the damaged mitochondria, cells usually undergo programmed death.⁴

In general, there are two approaches to induce cell apoptosis, *i.e.* the death receptor-mediated apoptosis and the intrinsic mitochondria pathway. The latter one encompasses a variety of key events including the release of caspase-activating proteins (cytochrome *c*), the depolarization of mitochondria with the loss of mitochondrial transmembrane potential, the disruption of electron transport and changes in energy metabolism, and participation the interaction with Bcl-2 family proteins.⁵ Thereby establishing mitochondria as targeted participants in active cell death is a new way to treat cancer.

Here, we propose to utilize peptide functionalized gold nanoparticles (AuNPs) to destroy mitochondria as the new anti-cancer strategy. AuNPs are selected as the nano-carriers due to their remarkable biocompatibility and non-toxicity, intrinsic stability, facile surface functionalization and potential therapeutic effect to cancer.⁶ In addition, AuNPs could significantly promote cellular

responses even without specific binding.⁷ The pro-apoptotic peptide (PAP) is used to functionalize AuNPs in that the α -helical PAP can cause a highly toxic effect and mitochondria-dependent programmed cell-death when internalized by the target cells.^{4b} By specifically damaging mitochondria, the hybrid PAP-AuNPs have promising applications in cancer treatments.

In this study, mono-dispersed AuNPs were fabricated by the classical Turkevich–Frens method.⁸ The α -helical amphipathic PAP was synthesized *via* standard Fmoc chemistry, and then conjugated with AuNPs to form PAP-AuNPs hybrid nanomaterial through the thiol–Au interaction (Scheme S1, ESI†).⁹ Transmission electron microscopy (TEM), dynamic light scattering (DLS), and UV-visible spectroscopy were used to monitor and analyze the stability and morphology changes of AuNPs after the PAP conjugation. The TEM image (Fig. S2a and S2b, ESI†) showed that both AuNPs and PAP-AuNPs have a favorable dispersion and their good stability was determined by DLS (Fig. S2e, ESI†). With the PAP conjugation, the zeta potential greatly increased from -35.8 mV (AuNPs) to 23.8 mV (PAP-AuNPs) (Table S1, ESI†). It is worth noting that the strong electrostatic repulsion force was the main force to stabilize AuNPs and PAP-AuNPs. UV-visible spectroscopy was further used to analyze surface plasmon resonance (SPR) and the results (Fig. S3a, ESI†) indicated that both AuNPs and PAP-AuNPs were stable in aqueous solution. Results from thermogravimetric analysis (TGA) showed that the content of peptide in PAP-AuNPs was around 21 wt% (Fig. S3b, ESI†). It is known that the biological activity of PAP is dependent upon its α -helical conformation.¹⁰ Therefore, Fourier transform infrared spectroscopy (FT-IR) and circular dichroism (CD) were employed to examine the conformation of PAP. As shown in Fig. S4 (ESI†), FT-IR and CD spectra confirmed that both PAP and PAP-AuNPs adopt the α -helical conformation.

Human cervical carcinoma (HeLa) cells were used as a model cell line to investigate the anti-cancer effect of PAP-AuNPs by MTT assay. As shown in Fig. S5 (ESI†), the half maximal inhibitory concentration (IC_{50}) of PAP is around 65 mg L⁻¹, while that of PAP-AuNPs is about 130 mg L⁻¹ (the PAP concentration is calculated as around 27.3 mg L⁻¹ based on the content of PAP-AuNPs determined by TGA analysis), indicating the cell

^a Key Laboratory of Biomedical Polymers of Ministry of Education & Department of Chemistry, Wuhan University, Wuhan 430072, P. R. China.

E-mail: xz-zhang@whu.edu.cn; Fax: +86 27 6875 4509; Tel: +86 27 6875 5993

^b Analysis and Testing Center, Institute of hydrobiology, Chinese Academy of Science, Wuhan 430072, P. R. China

† Electronic supplementary information (ESI) available: Details of experimental and supplementary figures. See DOI: 10.1039/c3cc43283a

‡ Those authors are equally contributed to this work.

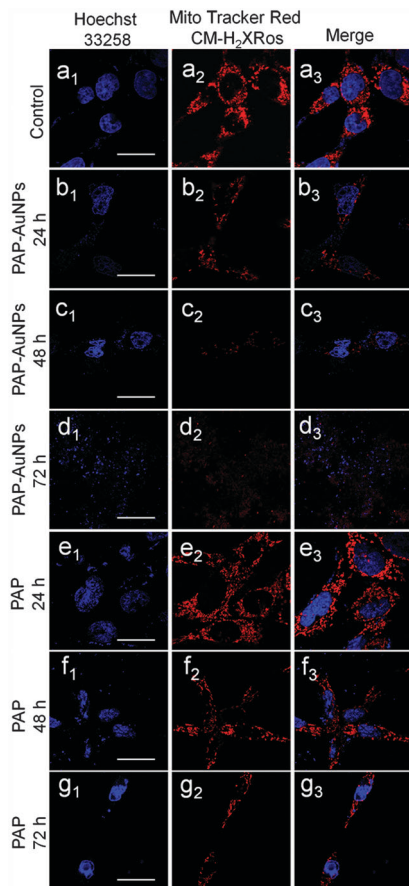


Fig. 1 Confocal laser scanning microscopy (CLSM) images of HeLa cells treated by PAP-AuNPs and PAP. Nuclei were stained by probe Hoechst 33258 and mitochondria were stained by probe Mito Tracker Red CM-H₂XRos. The red highlights are mitochondria. The scale bar was 20 μ m.

inhibition ability of PAP is enhanced when conjugated with AuNPs. As the control, the pure AuNPs did not exhibit obvious cytotoxicity.

Furthermore, to investigate and compare the mitochondria damaging ability of PAP-AuNPs and PAP, the mitochondria of HeLa cells were stained by a red fluorescence probe (Mito Tracker Red CM-H₂XRos). After incubation with HeLa cells, the red fluorescence decreases with time intervals (24, 48, and 72 h) for both PAP-AuNPs and PAP (Fig. 1). Moreover, the mitochondria reduction rate of the cells cultured with PAP-AuNPs is greater than that of cells cultured with equivalent PAP (Fig. 1b₂–d₂ compared with e₂, f₂, g₂, respectively). When the cells cultured with PAP-AuNPs for 72 h, only cell debris and tiny sporadic red fluorescence can be observed (Fig. 1d₂). However, some cells still remain intact and evident red fluorescence can still be found in the cells cultured with PAP (Fig. 1g₂). These results strongly indicate that the PAP-AuNPs have a much stronger capability to damage mitochondria than PAP.

In addition to the fluorescence studies shown above, TEM observation was further employed to investigate the cell uptake of PAP-AuNPs and morphology of mitochondria. After incubating HeLa cells with PAP-AuNPs for 4 h, a large number of PAP-AuNPs are internalized *via* endocytosis and the internalized PAP-AuNPs form endosomal vesicles (Fig 2a–c).¹¹ The mitochondria maintain

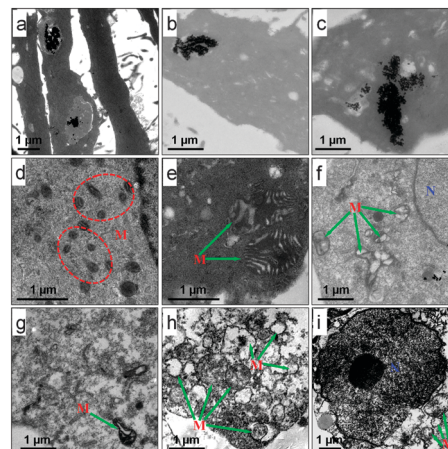


Fig. 2 Typical TEM images of HeLa cells uptake of PAP-AuNPs, such as (a), (b) and (c); from (d) to (h) reflect that PAP-AuNPs induce the mitochondrial morphology damage. The red M is symbol of mitochondria and the blue N is sign of nuclei.

a normal morphology at this time point (Fig. 2d). However, when incubation increased to 12 h and 24 h, the mitochondria lost their morphology and the cells reach complete apoptosis. After 12 h of incubation with PAP-AuNPs (Fig. 2e), the mitochondria in HeLa cells presented abnormal swelling and were devoid of condensed matrix content, the sporadic remnants of cristae can be observed. Except for a few mitochondria with the normal morphology (Fig. 2f), most mitochondria have been damaged with abnormal condensation and vacuolization. Progressive cellular damage could be found after 24 h of incubation, *i.e.*, the mitochondrion membrane is ruptured and the matrix has leaked out (Fig. 2g). As shown in Fig. 2h, profound damage occurred to mitochondria, *i.e.*, most of the mitochondria are damaged with the mitochondrial matrix leaking out. The structure of cristae could not be observed and the vacuoles formed. Even some cells are in a late apoptotic stage, extensive vacuolization mitochondria and the pyknotic, condensed nuclei could be obviously observed as the symbol of cell apoptosis, as demonstrated in Fig. 2i. TEM observations indicate that PAP-AuNPs can disrupt and damage the cancer cells mitochondria, leading to the apoptosis.

Mitochondrial transmembrane potential ($\Delta\Psi$ m) is an important parameter of mitochondrial functions and has been used to evaluate mitochondrial death. The damaging of mitochondria will lead to the depolarization of mitochondria with a drop in $\Delta\Psi$ m. Here, mitochondrial fluorescence probe JC-1 was used to study the mechanism of mitochondrial-regulated apoptosis, and JC-1 is a unique cationic dye that is used to determine the loss of $\Delta\Psi$ m. For healthy cells, the mitochondrial membrane presents a high $\Delta\Psi$ m; JC-1 will accumulate as a green monomer in the cytoplasm. Above the critical concentration, JC-1 could enter mitochondria and form J-aggregates with red fluorescence. However, in apoptotic cells, $\Delta\Psi$ m is relatively low, JC-1 could not accumulate in mitochondria and always stay in the cytoplasm as a green monomeric form.¹² As shown in Fig. 3, it can be found that J-monomer green fluorescence (Fig. 3a₁, b₁, c₁) increases gradually and red J-aggregates (Fig 3a₂, b₂, c₂) decrease simultaneously with the increase of the incubation time. After 72 h incubation, the red fluorescence of J-aggregates

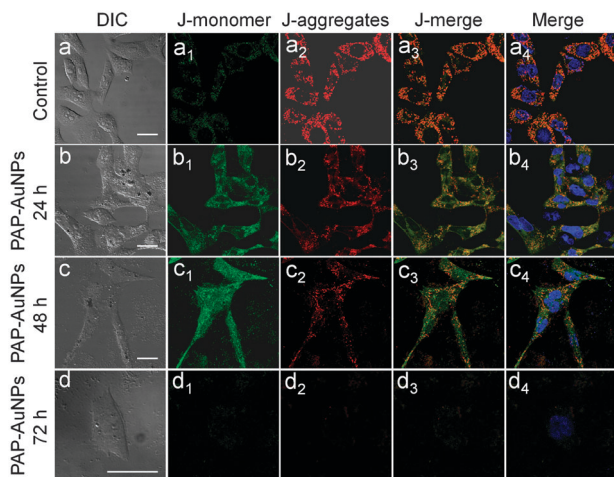


Fig. 3 CLSM images of HeLa cells incubated with PAP-AuNPs. Nuclei were stained by Hoechst 33258 and mitochondria were stained by JC-1 fluorescence probe. The scale bar was 20 μm .

completely disappeared (Fig. 3d₂). Meanwhile, the green J-monomer fluorescence also faded (Fig. 3d₁) and the nuclei become condensed (Fig. 3d₄). In addition, as shown in DIC bright field, the cells collapse and become “thinner” (Fig. 3c and d compared with a and b respectively) since most of the mitochondria have been destroyed. With the damage to the mitochondria, the membrane permeability of the cells is enhanced, leading to the leakage of cytoplasm. In fact, the permeable state of cell membrane can be observed directly. As shown in Fig. S6 (ESI[†]), cell edges are ruptured and cytoplasm has penetrated out.

The flow cytometry was used to quantitatively mark the cell population with the low $\Delta\Psi\text{m}$ and proved that PAP-AuNPs have a stronger ability to induce cell apoptosis. As shown in Fig. S7 (ESI[†]), P2 represents the cell population with the low $\Delta\Psi\text{m}$, indicating those cells are in the apoptotic state and representing the cell apoptosis rate. After 72 h of incubation, approximately 36.7% cells had low $\Delta\Psi\text{m}$ for those incubated with PAP, but there were 54.1% cells with low $\Delta\Psi\text{m}$ for those incubated with PAP-AuNPs, which is much higher. Flow cytometry results described above quantitatively confirmed that the apoptosis of the cells incubated with PAP-AuNPs is significantly enhanced. PAP-AuNPs can specifically damage mitochondria and induce a collapse of mitochondrial membrane potential.

To further study the anti-cancer mechanism of PAP-AuNPs, we conducted an apoptosis assay of HeLa cells. As shown in Fig. S8A (ESI[†]), the cell apoptosis presents in a time-dependent manner. Particularly for cells incubated with PAP-AuNPs for 72 h, the percentage of apoptotic and necrotic cells is approximately

59%, which is much higher than the cells incubated with PAP (about 18%, as shown in Fig. S9, ESI[†]). To confirm the apoptosis pathway of PAP-AuNPs, apoptosis associated proteins have been also detected by western blot analysis. As shown in Fig. S8B (ESI[†]), significant differences in the release of cytochrome *c* and expression of caspase-3 were observed for the cells incubated with PAP or PAP-AuNPs. PAP-AuNPs can promote the release of cytochrome *c* and expression of caspase-3, thus resulting in cell apoptosis. Obviously, the apoptotic pathway is typically mitochondria-mediated.

In summary, pro-apoptotic peptide functionalized AuNPs were fabricated and PAP-AuNPs can amplify the cell apoptosis. PAP-AuNPs can induce the mitochondrial membrane swelling and burst of membrane with mitochondrial matrix leaking out. By specifically damaging the organelle of mitochondria, PAP-AuNPs can cause the dysfunction of mitochondria, and trigger mitochondria-dependent programmed cancer cell death, thus leading to complete cancer cell apoptosis. Interestingly, this work provides new insights into anti-cancer strategy and it may lead to advanced treatment to cancers.

This work was supported by National Natural Science Foundation of China (51003079, 51125014, 51233003) and National Key Basic Research Program of China (2011CB606202).

Notes and references

- 1 V. P. Torchilin, *Annu. Rev. Biomed. Eng.*, 2006, **8**, 343.
- 2 C. S. Lim, *Adv. Drug Delivery Rev.*, 2007, **59**, 697.
- 3 (a) L. Rajendran, H. J. Knölker and K. Simons, *Nat. Rev. Drug Discovery*, 2010, **9**, 29; (b) B. Kang, M. A. Mackey and M. A. El-Sayed, *J. Am. Chem. Soc.*, 2010, **132**, 1517; (c) S. V. Boddapati, G. G. M. D'Souza, S. Erdogan, V. P. Torchilin and V. Weissig, *Nano Lett.*, 2008, **8**, 2559.
- 4 (a) A. Szewczyk and L. Wojtczak, *Pharmacol. Rev.*, 2002, **54**, 101; (b) H. M. Ellerby, W. Arap, L. M. Ellerby, R. Kain, R. Andrusiak, G. D. Rio, S. Krajewski, C. R. Lombardo, R. Rao, E. Ruoslahti, D. E. Bredesen and R. Pasqualini, *Nat. Med.*, 1999, **5**, 1032.
- 5 (a) D. R. Green and J. C. Reed, *Science*, 1998, **281**, 1309; (b) T. Xia, C. S. Jiang, L. J. Li, C. H. Wu, Q. Chen and S. S. Liu, *FEBS Lett.*, 2002, **510**, 62; (c) G. Kroemer, L. Galluzzi and C. Brenner, *Physiol. Rev.*, 2007, **87**, 99.
- 6 (a) E. Boisselier and D. Astruc, *Chem. Rev.*, 2009, **109**, 1759; (b) R. A. Sperling, P. R. Gil, F. Zhang, M. Zenella and W. J. Parak, *Chem. Rev.*, 2008, **108**, 1896; (c) G. F. Paciotti, D. G. I. Kingston and L. Tamarkin, *Drug Dev. Res.*, 2006, **67**, 47.
- 7 (a) B. D. Chithrani, A. A. Ghazani and W. C. W. Chan, *Nano Lett.*, 2006, **6**, 662; (b) H. K. Patra, S. Banerjee, U. Chaudhuri, P. Lahiri and A. K. Dasgupta, *Nanomed.: Nanotechnol., Biol. Med.*, 2007, **3**, 111; (c) E. C. Cho, Q. Zhang and Y. N. Xia, *Nat. Nanotechnol.*, 2011, **6**, 385.
- 8 (a) J. Turkevich, P. C. Stevenson and J. Hillier, *Discuss. Faraday Soc.*, 1951, **11**, 55; (b) G. Frens, *Nat. Phys. Sci.*, 1973, **241**, 20.
- 9 K. Eugenii and I. Willner, *Angew. Chem., Int. Ed.*, 2004, **43**, 6042.
- 10 M. M. Javadpour, M. M. Juban, W.-C. J. Lo, S. M. Bishop, J. B. Albery, S. M. Cowell, C. L. Becker and M. L. Mclaughlin, *J. Med. Chem.*, 1996, **39**, 3107.
- 11 P. Nativio, I. A. Prior and M. Brust, *ACS Nano*, 2008, **2**, 1639.
- 12 S. W. Perry, J. P. Norman, J. Barbieri, E. B. Brown and H. A. Gelbard, *BioTechniques*, 2011, **50**, 98.